Supplementary Information: A. Kocabas *et al.*

Material and Methods

Strains were grown and maintained under standard conditions[2] unless indicated otherwise. Transgenic lines with *pha-1* selection marker were grown under 24°C[22]. All optical stimulation experiments were done in *lite-1* mutants to minimize the animal's sensitivity to blue light[23]. A complete strain list and information on transgenes are included in the Supplementary Table 2.

Chemotaxis analysis

The animals' chemotaxis to a bacterial lawn were assayed on an open-lid, 10 cm nematode growth medium (NGM) plate incubated in room temperature overnight with 10 µL *Escherichia coli* OP50 at the center. N2 young adults were placed on the plate, 1.5 cm away from the center of the bacterial lawn. The animals' behaviors were recorded under 6x magnification by an EMCCD camera at 20Hz and analyzed by customized LabView scripts.

Odor stimulation setup

An N2 young adult was placed on an open-lid, food-free, 10 cm NGM plate for at least 1 minute. An electric valve (Supplementary Fig. 1b) was used to determine whether the air (100

sccm) was bubbled through water or 10^{-3} M isoamyl alcohol based on the posture of the freely moving animal. The images were recorded under 6x magnification by an EMCCD camera at 20 Hz and analyzed by customized LabView scripts.

Single neuron stimulation setup: L4 animals were transferred to a new NGM plate with a thin layer of *E. coli* OP50, containing 100 μM ATR (all-*trans* retinal, the co-factor required for functional light-gated ion channels)[16] if required, 24 hours before experiments in room temperature. An animal then was placed on an open-lid, food-free, 6 cm NGM plate for at least 1 minute. Dark-field 660 nm illumination was used to visualize the posture of the animal under 1x magnification by a video camera at 20 Hz (Fig. 2a, computer 2). Low-power 540 nm (0.1 mW/mm^2) epifluorescent illumination was used to visualize the neurons co-expressing light-gated ion channels and monomeric Kusabira-Orange (mKO)[24] at 15x by an EMCCD camera at 40 Hz (computer 1). Image thresholding and particle detection were used as the image processing algorithms to identify the mKO-tagged neurons. As the animal swung its head, the neurons in the field rotated and changed their positions. To offset the rotation effect, positions of the neurons were measured using the principle axis and the distance from the center of mass of the processed image. The processed images were then used to track the animal and to position the DLP mirrors to deliver light (4 mW/mm^2, 480 or 540 nm) on the neurons of interest with any desired temporal patterns to excite or inhibit the activity of the neurons. Feedback between motorized stage, DLP mirrors and image processing software was operated at 40 frames/sec to achieve a 5 μm spatial resolution of excitation on a freely moving animal. The images were processed, recorded, and analyzed by customized LabView scripts.

Reversal frequency

L4 animals were transferred to a new NGM plate with a thin layer of *E. coli* OP50, containing 100 μM ATR if required, 24 hours before experiments in room temperature. A 6 cm copper ring was placed in an open-lid, food-free, 10 cm NGM plate immediately before experiments to keep the animals in the field of view. Young adults then were transferred to the assay plate for 1 minute before the experiment started. The desired wavelength of light (1 mW/mm^2, 480 nm or 540 nm) was delivered in alternate 3-minute intervals for 1 hour using customized LabView scripts. The experiments were recorded by a video camera at 20 Hz. Reversal frequency was calculated from pirouettes determined by an automated worm tracker (http://wormsense.stanford.edu/tracker)[25].

Virtual light gradient setup: An AIY::*ChR2* animal was placed on an open-lid, food-free, 10 cm NGM plate for at least 1 minute before starting the experiment. A virtual-gradient of light, $I(r) = \exp\left(-r^2 / r_0^2\right)$, from 0 to 1 mW/mm^2 over 1.3 mm, where r_0=0.8 mm, was defined in an x-y coordinate system tied to the center of mass of the animal which was always at the center of the gradient profile (0.65 mm, 0.65 mm) (Supplementary Fig. 7a). The virtual light gradient moved with the center of mass of the animal but at a fixed orientation. At each time t, the coordinates of the nose tip were identified to calculate the corresponding intensity of light $I(n_x, n_y)$ (Fig. 4a). The animal was then illuminated with blue (480 nm) light at intensity $I(n_x, n_y)$, and thus, AIY instantaneously experienced the intensity of light at the nose tip.

Molecular biology

Arch::*EGFP*[14] was cloned into Fire lab vector kit plasmid *pPD96.52* (ligation number L2534, Addgene plasmid 1608). *Chop-2(H134R)::TagRFP* was obtained by swapping *TagRFP* with *YFP* in the previously cloned *chop-2(H134R)::YFP*[16]. *Arch::TagRFP* and *Arch::mKO* were

obtained respectively by swapping *TagRFP*[26] or *mKO*[24] with *EGFP* in *Arch::EGFP*. *TagRFP* and *GCaMP-3*[27] were codon-optimized for *C. elegans* (*de novo* synthesized by GenScript) whereas others were optimized for mammalian cells. We amplified 2kb *str-2p*[28], 1kb *ttx-3p*[29], 3kb *npr-9p*[30], 4.5kb *ser-2prom2*[31], and 2.4kb *odr-2(18)p*[32] by PCR from *C. elegans* genomic DNA. All the promoters were then fused with desired light-gated ion channels by PCR fusion[33].

Supplementary Table 1. Literature of behavioral defects upon inter- and motor-neuron ablations

Ablated neurons	Behavioral defects
AIB	reversals and omega turns decreased[7]
AIY	persistent reversals and omega turns, unclear about gradual turning[3,4,7]
AIZ	reversals decreased[17], gradual turning abolished[4]
RIB	reversal frequency and omega turns increased[3,7]
RIV	omega turns decreased, eliminates ventral bias of omega turns[7]
RIM	reversals decreased[3,7]
AVA	reversals decreased[7]
AVB	reversals increased[34]
AVA + AVD	inability to move backward[34]
AVB + PVC	inability to move forward[34]
SMB	head-bending angle increased, loopy and high-amplitude sinusoidal movement[7]
SMD	omega turns reduced, reversal frequency increased, amplitude of omega turn decreased[7]
RMD	reversal frequency increased[7]
RME	head bending angle increased, loopy movement[21]

Supplementary Table 2. Transgenic strains, genotypes, and expression.

Name	Genotype	Expression
SRS167	*pha-1(e2123)* III; *lite-1(ce314)* X	N/A
SRS301	*sraEx301 [str-2p::chop-2(H134R)::TagRFP; str-2p::TagRFP; pBX];* *pha-1(e2123)*III*; lite-1(ce314)* X	AWC^{ON}, (ASI)*[28]
SRS230	*sraEx230[str-2p::Arch::TagRFP; pBX];* *pha-1(e2123)*III*; lite-1(ce314)* X	AWC^{ON}, (ASI)[28]
SRS281	*sraEx281[ttx-3p::chop-2(H134R)::TagRFP; pBX];* *pha-1(e2123)*III*; lite-1(ce314)* X	AIY[29]

SRS279	*sraEx279[ttx-3p::Arch::TagRFP; pBX]; pha-1(e2123)*III*; lite-1(ce314)* X	AIY[29]
SRS291	*sraEx291[npr-9p::chop-2(H134R)::TagRFP; pBX]; pha-1(e2123)*III*; lite-1(ce314)* X	AIB[30]
SRS278	*sraEx278[npr-9p::Arch::TagRFP; pBX]; pha-1(e2123)*III*; lite-1(ce314)* X	AIB[30]
SRS306	*sraEx306 [ser-2prom2::chop-2(H134R)::TagRFP; ser-2prom2::mKO; pBX]; pha-1(e2123)*III; *lite-1(ce314)* X	AIY, AIZ, RME, DVA, BDU, [RID]**, [SIA], (PVT)[31]
SRS329	*sraEx329[odr-2(18)p::chop-2(H134R)::TagRFP; odr-2(18)p::mKO; pBX]; pha-1(e2123)*III; *lite-1(ce314)* X	SMB, [RME], ALN, PLN, [RIG][32]
SRS392	*njIS10[glr-3p::GFP]; sraEX112[ttx-3p::chop-2(H134R); unc-122::mCherry]; sraEX392[ser-2prom2::mKO]; lite-1(ce314)* X	GFP: RIA[35]; mCherry: coelomocytes[36], AIY[29]; mKO: AIY, AIZ, RME, DVA, BDU, [RID]**, [SIA], (PVT)[31]

* Neurons in the parentheses indicate weak or unstable expression in both the reporter lines in literature and the transgenic lines that we generated.
**Neurons in the square brackets indicate weak or unstable expression in the transgenic lines we generated.

Movie Captions

Movie S1: Asymmetric odor stimulation causes turning.

Movie of an animal in the setup in Supplementary Fig. 1b exposed to asymmetric odor stimulation. Appearance of blue dot indicates when vapors of isoamyl alcohol were blown on the entire animal, and "Dorsal Stimulation" or "Ventral Stimulation" indicates asymmetric dorsal or ventral stimulation. The movie shows that the animal turned in the direction in which its head was bent when the odor was delivered.

Movie S2: Asymmetric excitation of AIY causes turning.

Movie of asymmetric excitation of AIY in a *pttx-3::ChR2* animal with blue (480 nm) light. Appearance of blue dot indicates the animal was exposed to light. "Dorsal Stimulation" or

"Ventral Stimulation" indicates asymmetric dorsal or ventral excitation. The movie shows that the animal turned in the direction in which its head was bent when AIY were excited.

Movie S3: Asymmetric excitation of the AIY interneurons in an animal co-expressing ChR2 and mKO in AIY, AIZ, and RME causes turning.

We validated the spatial resolution of our system (Fig. 2a) by asymmetric excitation of AIY interneurons in an animal co-expressing ChR2 and mKO in AIY, AIZ and RME under the control of *ser-2prom2*. The top left panel shows the animal under dark-field illumination gathered by the video camera. The top middle panel shows the 15x magnification fluorescence image of the neurons gathered by the EMCCD camera using 540 nm illumination, which excited mKO. The image was processed to identify AIY (bounded by a blue rectangle), which were specifically excited by 480 nm using DLP mirror arrays. When AIY were excited, AIY intensity increased because of emission from mKO. The top right panel shows the trajectory of the animal during the experiment. The bottom panel shows the intensity of AIY as a function of time during the experiment (Supplementary Fig. 2g). During the initial part of the movie, asymmetric dorsal excitation of AIY caused a dorsal, counterclockwise turn. In the later part of the movie (after a period of no excitation of AIY), asymmetric ventral excitation of AIY caused a ventral, clockwise turn. The movie shows that the animal turned in the direction in which its head was bent when AIY were excited. Thus, the system can asymmetrically excite AIY in the presence of other neurons and reproduce the results from asymmetrically excite AIY in animals only express ChR2 in AIY (Fig. 2b, Supplementary Movie 2).

Movie S4: Asymmetric inhibition of AIY causes turning.

Movie of asymmetric inhibition of AIY in a *pttx-3*::*Arch* animal with green (540 nm) light. Appearance of green dot indicates the animal was exposed to light. "Dorsal Stimulation" or

"Ventral Stimulation" indicates asymmetric dorsal or ventral inhibition. The movie shows that the animal turned in the direction opposite to the one in which its head was bent when AIY were inhibited.

Movie S5: Symmetric excitation of AIY inhibits reversals.

Symmetric excitation of AIY::*ChR2* in a *pttx-3::ChR2* animal with constant blue (480 nm) light inhibits reversals. Presence of light is indicated by a blue dot. In the absence of light, the animal reversed more frequently, and in the presence of light, it did not reverse.

Movie S6: Asymmetric excitation of AIZ causes turning in the direction opposite to that in animals with asymmetric excitation of AIY.

Asymmetric excitation of just the AIZ interneuron pair with blue (480 nm) light in an animal co-expressing ChR2 and mKO in AIY, AIZ and RME (*ser-2prom2::ChR2; ser-2prom2::mKO*) is shown. The top left panel shows the animal under dark-field illumination gathered by the video camera (Fig. 2a). The top middle panel shows the 15x magnification fluorescence image of the neurons gathered by the EMCCD camera under 540 nm illumination, which excited mKO. The image was processed to identify AIZ (bounded by a blue rectangle) and the animal was excited by 480 nm light specifically on AIZ using DLP mirror arrays. When AIZ were excited, AIZ intensity increased because of emission from mKO. The top right panel shows the trajectory of the animal during the experiment, with the blue parts of the trajectory denoting the times when the light was on (Supplementary Fig. 5a, right). The bottom panel shows the fluorescence intensity of AIZ (blue), AIY (green), and RME (red) as a function of time during the experiment (Supplementary Fig. 5a, left). Asymmetric ventral excitation of AIZ caused a dorsal, counterclockwise turn. The movie shows that the animal turned in the direction opposite to that in which its head was bent when AIZ were excited.

Movie S7: Asymmetric excitation of motor neurons SMB causes turning.

Asymmetric excitation of just the SMB interneurons with blue (480 nm) light in an animal co-expressing ChR2 and mKO in SMB and other neurons in the nerve ring (*podr-2(18)::ChR2; podr-2(18)::mKO*) is shown. The top left panel shows the animal under dark-field illumination gathered by the video camera (Fig. 2a). The top right panel shows the 15x magnification fluorescence image of the neurons gathered by the EMCCD camera under 540 nm illumination, which excited mKO. The image was processed to identify SMB (bounded by a blue rectangle) and the animal was excited by 480 nm light specifically on SMB using DLP mirror arrays. When SMB were excited, SMB intensity increased because of emission from mKO. The bottom panel shows the fluorescence intensity of SMB (blue) as a function of time during the experiment (Supplementary Fig. 5b, right). The movie shows that asymmetric ventral excitation of SMB caused ventral, counterclockwise turns (Supplementary Fig. 5b, left).

Movie S8: Asymmetric excitation of motor neurons RME causes turning.

Asymmetric excitation of just the RME interneurons with blue (480 nm) light in an animal co-expressing ChR2 and mKO in AIY, AIZ and RME in the nerve ring (*ser-2prom2::ChR2; ser-2prom2::mKO*) is shown. The top left panel shows the animal under dark-field illumination gathered by the video camera (Fig. 2a). The top right panel shows the 15x magnification fluorescence image of the neurons gathered by the EMCCD camera under 540 nm illumination, which excited mKO. The image was processed to identify RME (bounded by a blue rectangle) and the animal was excited by 480 nm light specifically on RME using DLP mirror arrays. When RME were excited, RME intensity increased because of emission from mKO. The bottom panel shows the fluorescence intensity of RME (blue) as a function of time

during the experiment (Supplementary Fig. 5c, left). The movie shows that asymmetric ventral excitation of RME caused dorsal, counterclockwise turns (Supplementary Fig. 5c, right).

Movie S9: Asymmetric inhibition of the sensory neuron AWC^{ON} causes turning.

Movie of an AWC^{ON}::*Arch::mKO* animal under the control of *pstr-2* exposed to asymmetric inhibition with green (540 nm) light. Appearance of green dot indicates when the animal was exposed to light. Concomitantly, one could see the neuron AWC^{ON} because mKO was also excited by the same wavelength of light. "Dorsal Stimulation" or "Ventral Stimulation" indicates asymmetric dorsal or ventral stimulation. The movie shows that the animal turned in the direction in which its head was bent when AWC^{ON} was inhibited.

Movie S10: AIY::*ChR2* animal in a fixed light gradient cannot track the gradient direction.

Movie of an AIY::*ChR2* animal under the control of *pttx-3* crawling through a fixed spatial light gradient in an x-y coordinate system whose origin was tied to the center of mass of the animal so that the gradient moved with the animal but retained its orientation at 45 degrees to the x axis. The spatial profile of the intensity $I(r) = \exp(-r^2 / r_0^2)$, from 0 to 1 mW/mm^2 over 1.3 mm, where r_0 = 0.8 mm. The location of the peak of the gradient is colored by blue. See Supplementary Fig. 7a, c for gradient profile and tracks of individual animals in this gradient.

Movie S11: AIY::*ChR2* animal in a virtual light gradient tracks the gradient direction through repeated inversions of the gradient.

Movie of an AIY::*ChR2* animal under the control of *pttx-3* crawling through a virtual light gradient in an x-y coordinate system whose origin was tied to the center of mass of the animal. The excitation light intensity on AIY was dependent on the nose tip position of the animal

(Fig. 4a). The gradient moved with the animal and retained its orientation at 45 degrees to the x-axis. The spatial profile of the intensity $I(r) = \exp(-r^2 / r_0^2)$, from 0 to 1 mW/mm^2 over 1.3 mm, where r_0 = 0.8 mm (Supplementary Fig. 7a). The location of the peak of the gradient is colored by blue. The gradient was suddenly rotated by 180 degrees during the course of the movie, when this blue region occupied the opposite vertex.

Supplementary Figure Captions

Figure S1: Asymmetric odor stimulation causes the animal to turn.

a, The mean of the odor signal $I(t)$ at the animal's nose tip gradually increased as the animal in Fig. 1a approached the bacterial lawn. **b,** A closed-loop control system for odor delivery. Based on the animal's posture, obtained by automated image processing at 20Hz by a customized worm tracker, the computer controlled an electric valve to determine whether air was bubbled through 10^{-3} M isoamyl alcohol (red tube) or through water (blue tube) before being gently blown on the freely moving animal. **c,** Trajectory of the center of mass of an animal that first experienced asymmetric dorsal odor stimulation followed by asymmetric ventral odor stimulation showed a dorsal turn followed by a ventral turn. Red: no odor stimulation; green: odor stimulation. **d,** Sample trajectories of animals with no odor stimulation. Grey bar: mean turning angle; D: dorsal (positive turning angle); V: ventral (negative turning angle); F: front; B: back; n=10.

Figure S2: Using asymmetric AIY stimulation to validate the single-neuron stimulation setup.

a, An animal expressing ChR2 and mKO in neurons AIY, AIZ and RME is shown (*ser-2prom2::ChR2; ser-2prom2::mKO*) The relative positions of neurons AIY, AIZ, and RME changed as the animal crawled (left: 1x dark field image; right: corresponding 15x

fluorescence image of the neurons AIY, AIZ and RME). **b,** Distributions of *lite-1* mutant worm speeds measured on a food-free, NGM plate (n=18, t=60 min). **c-e,** The trajectories of animals expressing ChR2 in AIY and mKO in AIY, AIZ and RME (*pttx-3::ChR2; ser-2prom2::mKO*) exposed to asymmetric stimulation of (**c**) AIY::*ChR2*, (**d**) AIZ::*mKO*, or (**e**) RME::*mKO*. **f**, Turning angle of animals upon asymmetric stimulation of AIY::*ChR2* (n=5), AIZ::*mKO* (n=5) and RME::*mKO* (n=5) from (**c**) to (**e**). Dorsal: asymmetric dorsal stimulation. Ventral: asymmetric ventral stimulation. **, $p<0.05$, two-sample t-test. **g**, An animal co-expressing ChR2 and mKO in AIY, AIZ and RME (*ser-2prom2::ChR2; ser-2prom2::mKO*) exposed to asymmetric stimulation of AIY::*ChR2*. Time series plot of mKO fluorescence fold change (left) in AIY (blue line), AIZ (yellow), and RME (green) upon asymmetric AIY stimulation from t=50s onwards. AIY showed significant fluorescence fold change when 480nm light was focused on them but not otherwise. AIZ and RME did not show any increase in intensity. Before 102.4s, AIY experienced asymmetric dorsal stimulation (480 nm) and from 136.7s onwards AIY experienced asymmetric ventral stimulation. The trajectory of the animal (right) shows that asymmetric dorsal stimulation led to a dorsal turn (from 0s to 102.4s) and ventral stimulation to ventral turn (t = 136.7s onwards) (blue: high power 480 nm illumination excites ChR2 (4 mW/mm^2); green: low power 540 nm illumination that does not excite ChR2 (0.1 mW/mm^2) used for imaging

Figure S3: Using asymmetric AIY stimulation causes the animal to turn and changes the reversal frequency.

a, Sample tracks of AIY::*Arch* animals under the control of *ttx-3* promoter. The animals turned in the opposite direction in which its head was bent when AIY were inhibited. Left: asymmetric dorsal stimulation; right: asymmetric ventral stimulation. **b,** The trajectory of an animal with AIY::*ChR2* symmetric excitation showed no reversals (blue) when AIY were

stimulated and increased reversals (red) when AIY were not stimulated. Blue: 480 nm stimulation; red: no stimulation.

Figure S4: Asymmetric and symmetric AIB stimulation both regulate the reversal frequency but not gradual turns.

a, Sample tracks of AIB::*ChR2* animals under the control of *pnpr-9*. The animals reversed immediately upon stimulation but did not turn. Left: asymmetric dorsal stimulation; right: asymmetric ventral stimulation. **b,** Sample tracks of AIB::*Arch* animals under the control of *pnpr-9*. The animals did not turn. Left: asymmetric dorsal stimulation; right: asymmetric ventral stimulation. **c,** The number of reversals of AIB::*ChR2* animals fed without ATR (top, when the light-gated ion channels were not functional due to the absence of the crucial co-factor all-*trans* retinal) and with ATR (bottom) for sequential three minute intervals when 480 nm blue light was off (orange bars) and then on (blue bars) for three minutes to excite AIB. In the presence of ATR, animals showed increased reversals in the presence of light. **d,** The number of reversals of AIB::*Arch* animals fed without ATR (left) and with ATR (right) for sequential three minute intervals when 540 nm green light was off (orange bars) and then on (green bars) for three minutes to inhibit AIB. Animals with ATR showed decreased reversal frequency in the presence of light. **e,** Bars of reversal frequency difference between when the light was on compared to when it was off. (AIB::*ChR2* animals, n=14; AIB::*Arch* animals, n=11; **, $p<0.05$ in two-sample t-test).

Figure S5: Asymmetric stimulation of AIZ, SMB and RME causes turning.

a, An animal co-expressing ChR2 and mKO in AIY, AIZ and RME (*ser-2prom2::ChR2; ser-2prom2::mKO*) was exposed to asymmetric stimulation of AIZ::*ChR2*. Time series plot of mKO fluorescence fold change (left) in AIY (blue line), AIZ (yellow), and RME (green) upon

asymmetric AIZ stimulation showed significant fluorescence fold change when 480nm light was focused on them but not otherwise. AIY and RME did not show any increase in intensity. The trajectory of the animal (right) shows that asymmetric ventral stimulation led to a dorsal turn (blue: high power 480 nm illumination excites ChR2 (4 mW/mm^2); green: low power 540 nm illumination that does not excite ChR2 (0.1 mW/mm^2) used for imaging). **b**, An animal co-expressing ChR2 and mKO in SMB and other neurons in the nerve ring (p*odr-2(18)::ChR2; podr-2(18)::mKO*) was exposed to asymmetric stimulation of SMB::*ChR2*. Time series plot of mKO fluorescence fold change (left) in SMB (blue) and nerve ring (NR, yellow) upon asymmetric SMB stimulation showed significant fluorescence fold change when 480nm light was focused on them but not otherwise. The nerve ring did not show any increase in intensity. Gray bar: the animal was out of focus during this period. The middle panel showed the expression pattern of *podr-2(18),* expressing ChR2 and mKO in SMB and nerve ring. The trajectory of the animal (right) shows that asymmetric dorsal stimulation led to dorsal turns. **c**, An animal co-expressing ChR2 and mKO in AIY, AIZ and RME (*ser-2prom2::ChR2; ser-2prom2::mKO*) was exposed to asymmetric stimulation of RME::*ChR2*. Time series plot of mKO fluorescence fold change (left) in AIY (blue line), AIZ (yellow) and RME (green) upon asymmetric RME stimulation showed significant fluorescence fold change when 480nm light was focused on them but not otherwise. AIY and AIZ did not show any increase in intensity. The trajectory of the animal (right) shows that asymmetric ventral stimulation led to a dorsal turn. **d,** Sample tracks of RME::*ChR2* animals under the control of *ser-2prom2*. The animals turned in the opposite direction in which its head was bent when RME were excited. Left: asymmetric dorsal stimulation; middle: no stimulation; right: asymmetric ventral stimulation.

Figure S6: Asymmetric AWC^{ON} stimulation causes the animal to turn and symmetric AWC^{ON} stimulation regulates the reversal frequency.

a, **b,** Sample tracks of animals. Left: asymmetric dorsal stimulation; right: asymmetric ventral stimulation. (**a**) AWC^{ON}::*ChR2* animals under the control of *pstr-2*. (**b**) AWC^{ON}::*Arch* animals under the control of *pstr-2*. **c,** The number of reversals of AWC^{ON}::*ChR2* animals without ATR (top) and with ATR (bottom) for sequential three minute intervals when 480 nm blue light was off (orange bars) and then on (blue bars) to excite AWC^{ON}. Animals showed increased reversals in the presence of light when they were fed ATR. **d,** The number of reversals of AWC^{ON}::*Arch* animals fed without ATR (left) and with ATR (right) for sequential three minute intervals when 540 nm green light was off (orange bars) and then on (green bars) to inhibit AWC^{ON} in the presence of ATR showed decreased reversals in the presence of light. **e,** Bars of reversal frequency difference between when the light was on and when it was off (AWC^{ON}::*ChR2* animals, n=21; AWC^{ON}::*Arch* animals, n=19; **, $p<0.05$ in two-sample t-test).

Figure S7: Fixed light gradient cannot elicit chemotactic behavior.

a, The profile of the light gradient $I(r) = \exp(-r^2 / r_0^2)$, from 0 to 1 mW/mm^2 (pseudocolor) across 1.3 mm, where r is the distance from the peak of the gradient and r_0 = 0.8 mm. **b,** Superposition of the bright field and fluorescence image of a nematode co-expressing ChR2 and mKO in AIY under the control of *ttx-3* promoter showed that the somas of AIY were behind the nose tip by 150 μm. **c,** Trajectories of AIY::*ChR2* animals (n=10) moving in a fixed spatial light gradient direction at 45 degrees (arrow direction) could not stably track the gradient direction.

Supplementary References

22 Granato, M., Schnabel, H. & Schnabel, R. pha-1, a selectable marker for gene transfer in C. elegans. *Nucleic Acids Res* **22**, 1762-1763 (1994).

23 de Bono, M. *et al.* A Novel Molecular Solution for Ultraviolet Light Detection in Caenorhabditis elegans. *PLoS Biology* **6**, e198, doi:10.1371/journal.pbio.0060198 (2008).

24 Karasawa, S., Araki, T., Nagai, T., Mizuno, H. & Miyawaki, A. Cyan-emitting and orange-emitting fluorescent proteins as a donor/acceptor pair for fluorescence resonance energy transfer. *Biochem J* **381**, 307-312, doi:10.1042/BJ20040321 [pii] (2004).

25 Aramayo, R. *et al.* The Parallel Worm Tracker: A Platform for Measuring Average Speed and Drug-Induced Paralysis in Nematodes. *PLoS ONE* **3**, e2208, doi:10.1371/journal.pone.0002208 (2008).

26 Merzlyak, E. M. *et al.* Bright monomeric red fluorescent protein with an extended fluorescence lifetime. *Nat Methods* **4**, 555-557, doi:nmeth1062 [pii] 10.1038/nmeth1062 (2007).

27 Hires, S. A., Tian, L. & Looger, L. L. Reporting neural activity with genetically encoded calcium indicators. *Brain Cell Biology* **36**, 69-86, doi:10.1007/s11068-008-9029-4 (2008).

28 Troemel, E. R., Sagasti, A. & Bargmann, C. I. Lateral signaling mediated by axon contact and calcium entry regulates asymmetric odorant receptor expression in C. elegans. *Cell* **99**, 387-398, doi:S0092-8674(00)81525-1 [pii] (1999).

29 Hobert, O. *et al.* Regulation of interneuron function in the C. elegans thermoregulatory pathway by the ttx-3 LIM homeobox gene. *Neuron* **19**, 345-357, doi:S0896-6273(00)80944-7 [pii] (1997).

30 Bendena, W. G. *et al.* A Caenorhabditis elegans allatostatin/galanin-like receptor NPR-9 inhibits local search behavior in response to feeding cues. *Proc Natl Acad Sci U S A* **105**, 1339-1342, doi:0709492105 [pii] 10.1073/pnas.0709492105 (2008).

31 Tsalik, E. LIM homeobox gene-dependent expression of biogenic amine receptors in restricted regions of the C. elegans nervous system. *Developmental Biology* **263**, 81-102, doi:10.1016/s0012-1606(03)00447-0 (2003).

32 Chou, J. H., Bargmann, C. I. & Sengupta, P. The Caenorhabditis elegans odr-2 gene encodes a novel Ly-6-related protein required for olfaction. *Genetics* **157**, 211-224 (2001).

33 Boulin, T. Reporter gene fusions. *WormBook*, doi:10.1895/wormbook.1.106.1 (2006).

34 Chalfie, M. *et al.* The neural circuit for touch sensitivity in Caenorhabditis elegans. *J Neurosci* **5**, 956-964 (1985).

35 Brockie, P. J., Madsen, D. M., Zheng, Y., Mellem, J. & Maricq, A. V. Differential expression of glutamate receptor subunits in the nervous system of Caenorhabditis elegans and their regulation by the homeodomain protein UNC-42. *The Journal of neuroscience : the official journal of the Society for Neuroscience* **21**, 1510-1522 (2001).

36 Loria, P. M., Hodgkin, J. & Hobert, O. A conserved postsynaptic transmembrane protein affecting neuromuscular signaling in Caenorhabditis elegans. *The Journal of neuroscience : the official journal of the Society for Neuroscience* **24**, 2191-2201, doi:10.1523/JNEUROSCI.5462-03.2004 (2004).

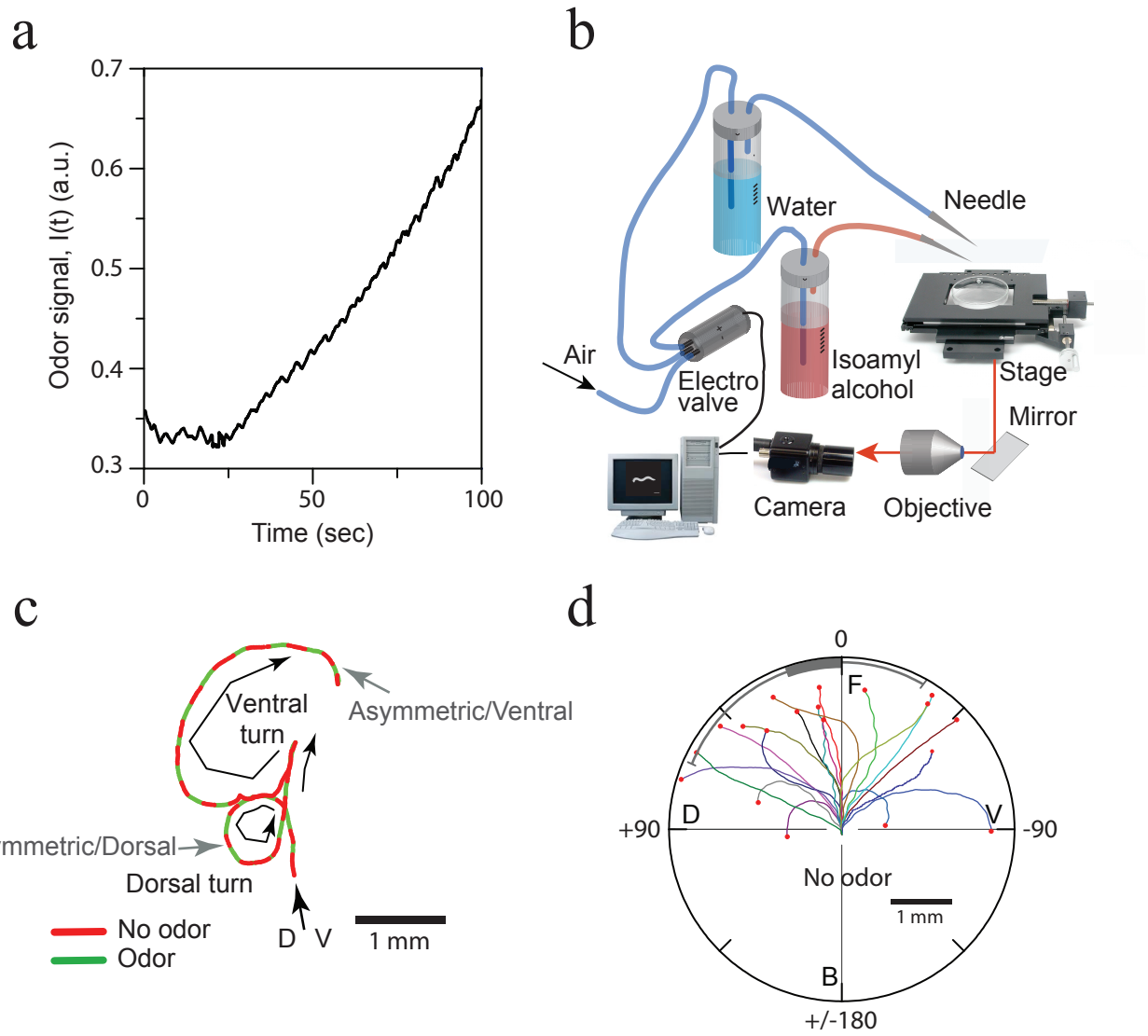

Figure S1 *Ramanathan*

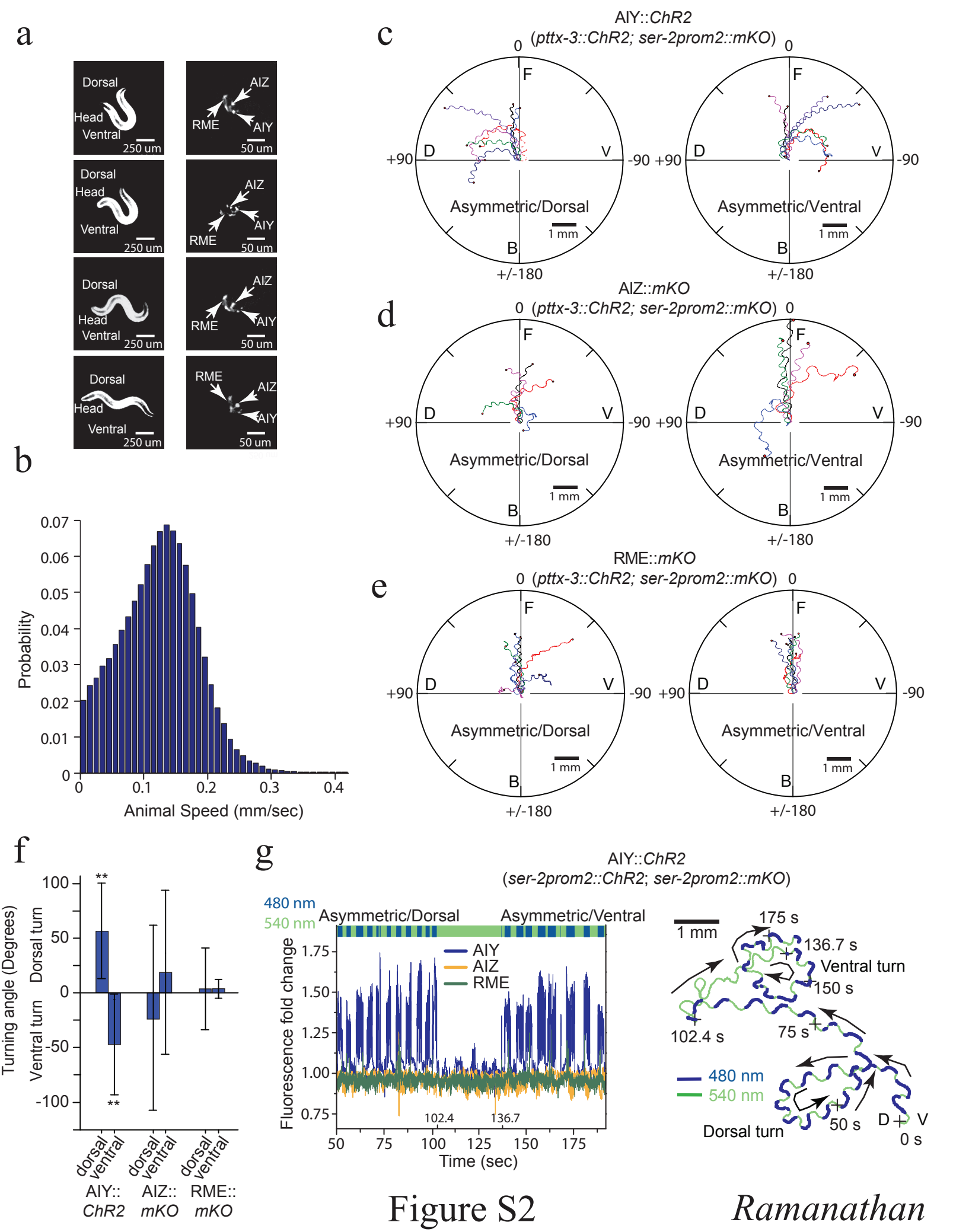

Figure S2

Ramanathan

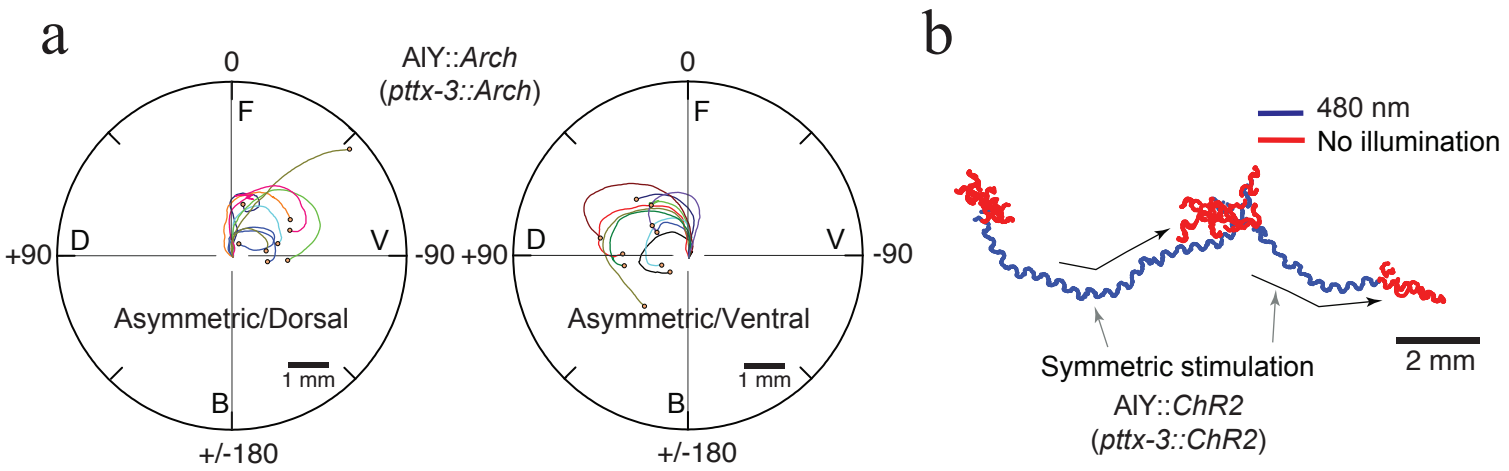

Figure S3 *Ramanathan*

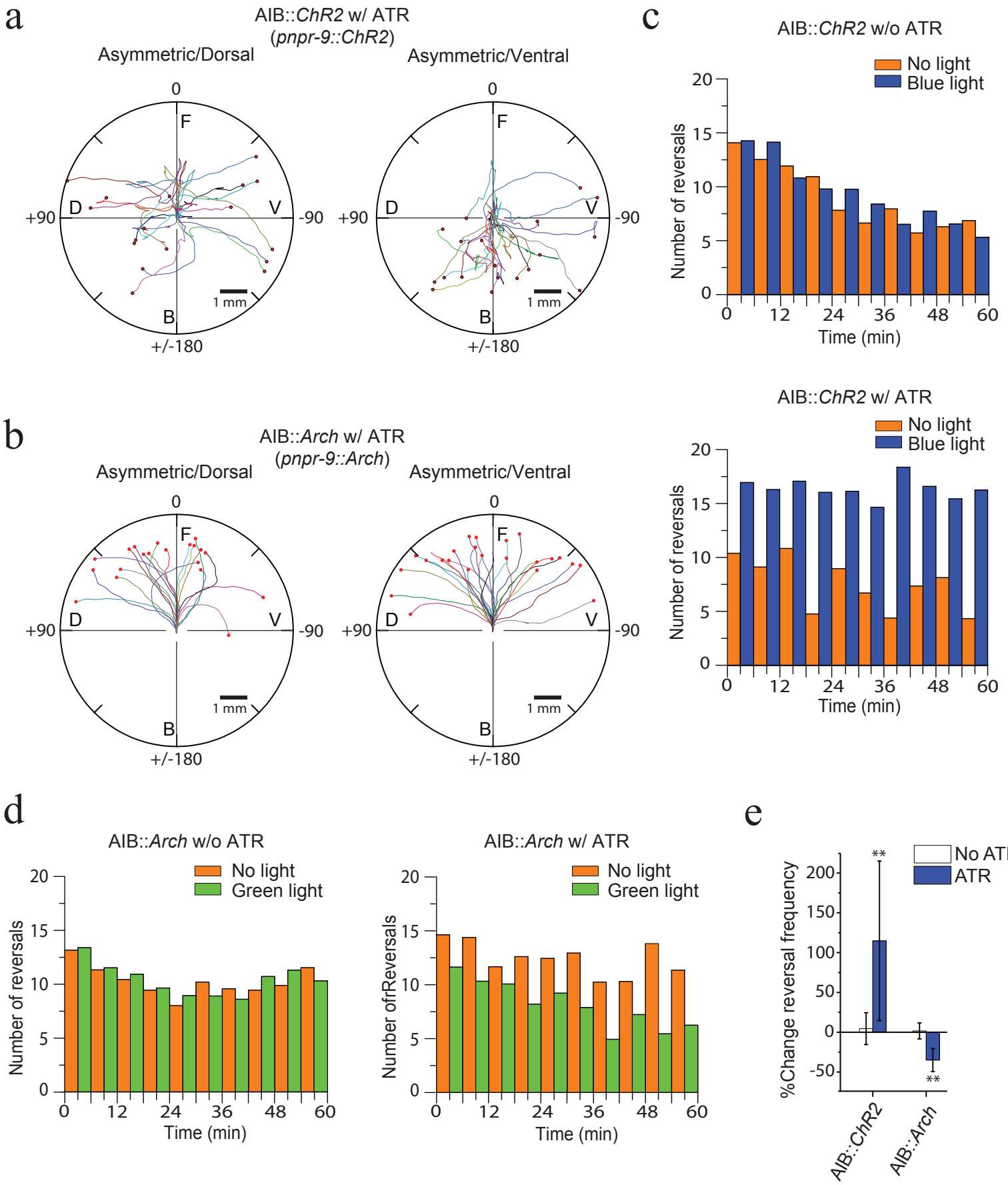

Figure S4

Ramanathan

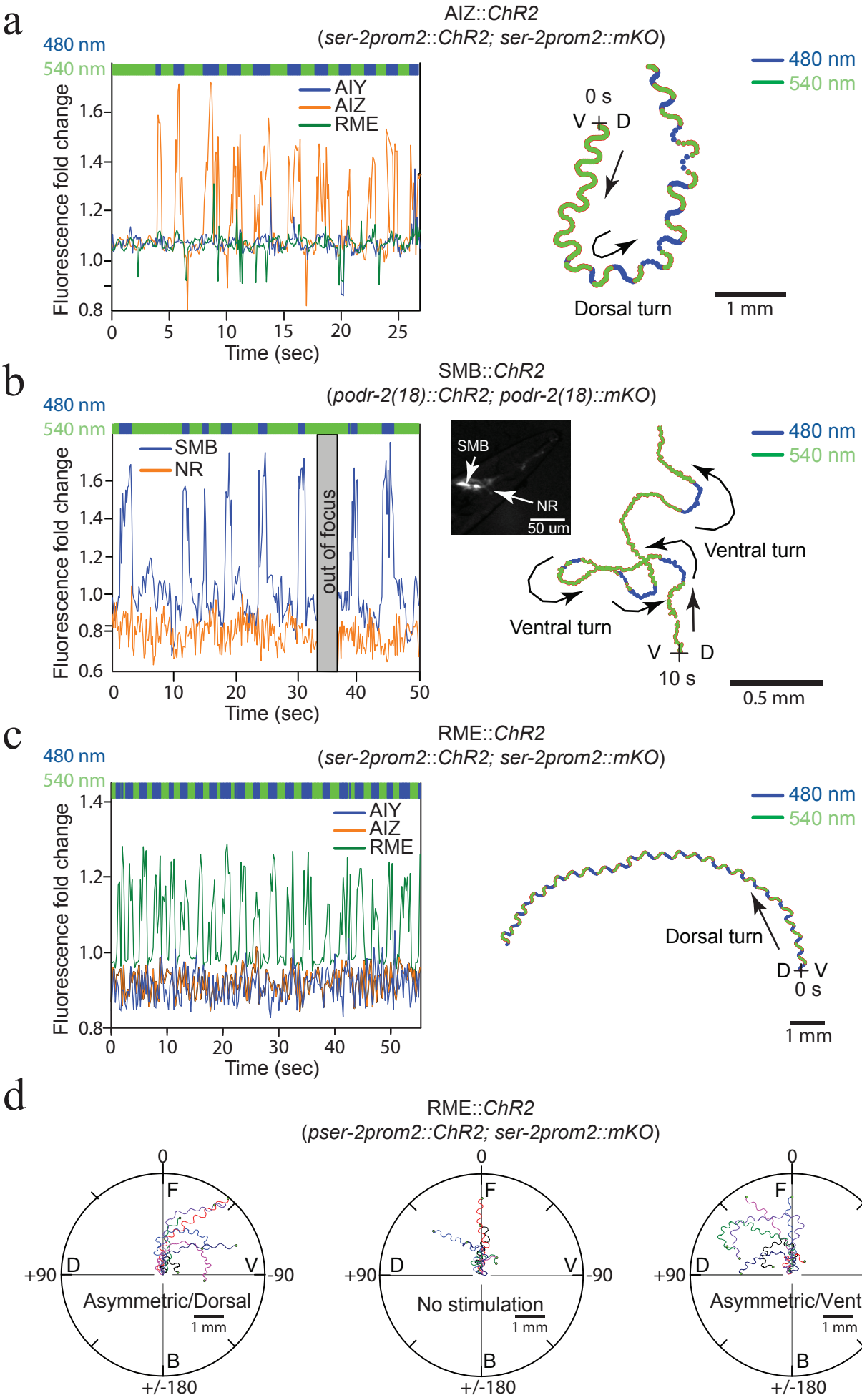

Figure S5 *Ramanathan*

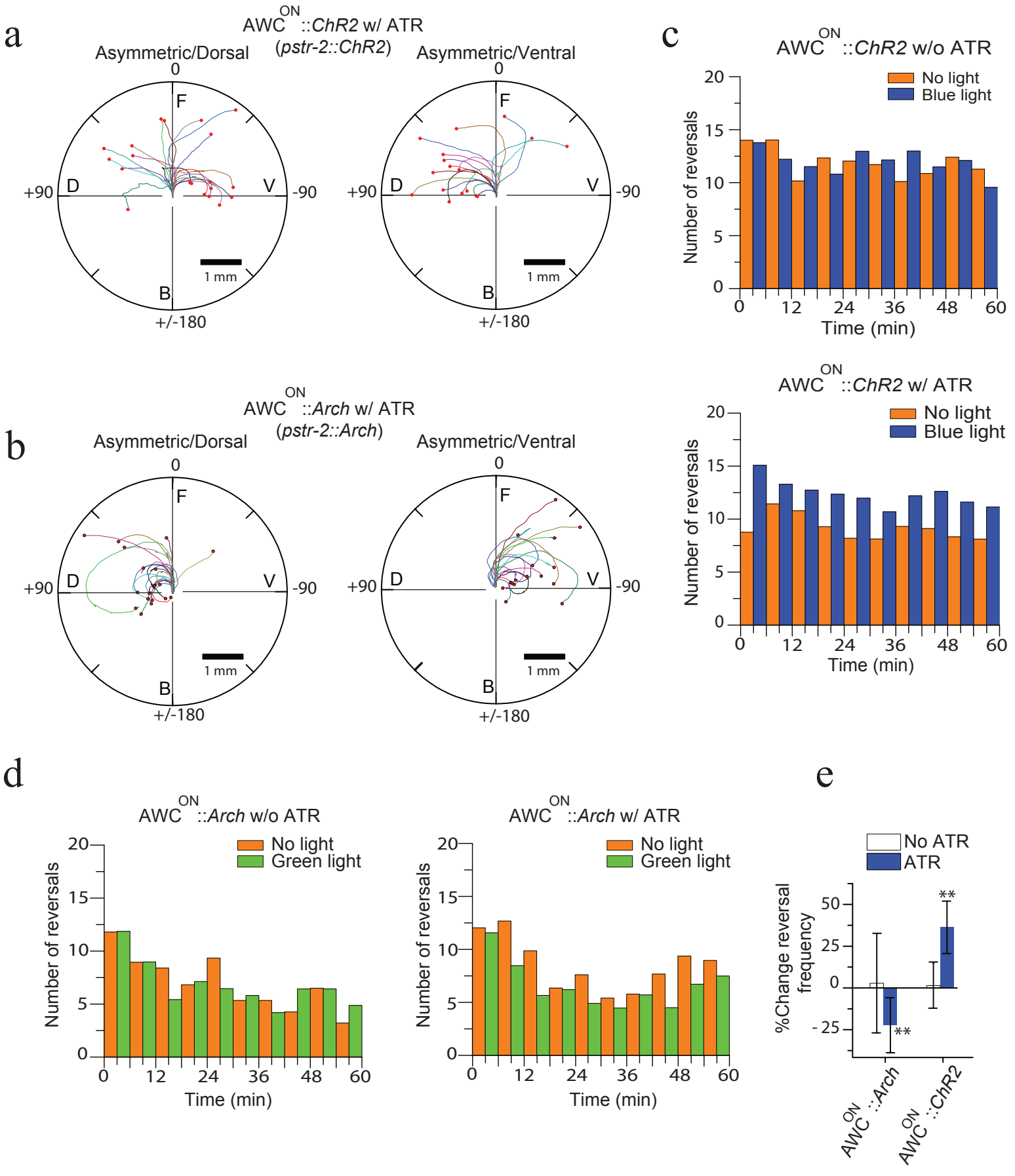

Figure S6

Ramanathan

a

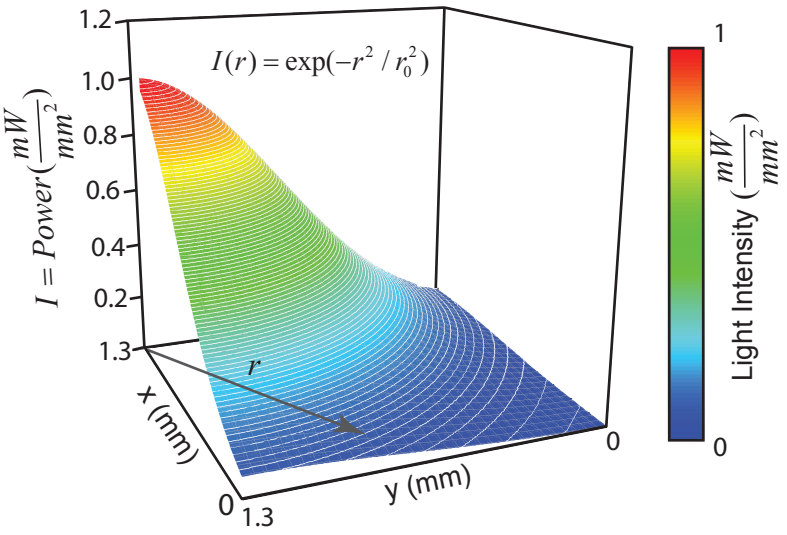

b

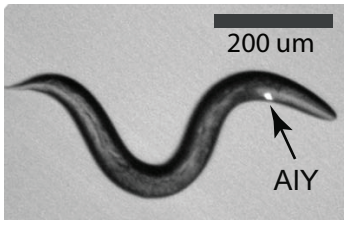

c

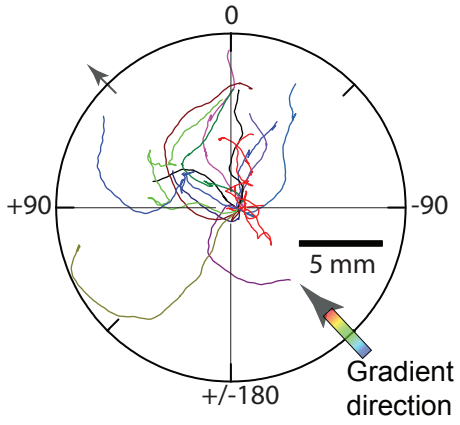

Figure S7 *Ramanathan*